

Research Article

Synthesis and Infrared Performance of SiB₆ Powder through “Chemical Oven” Self-Propagating Combustion

Shuang Shuang ¹, Fengxia Yang,^{1,2} Zhiwei Li,² Jiangtao Li,¹ and Xiangmin Meng³

¹Key Laboratory of Cryogenics, Technical Institute of Physics and Chemistry, Chinese Academy of Sciences, Beijing 100190, China

²University of Chinese Academy of Sciences, Beijing 100049, China

³Key Laboratory of Photochemical Conversion and Optoelectronic Materials, Technical Institute of Physics and Chemistry CAS, Beijing 100190, China

Correspondence should be addressed to Shuang Shuang; shuangshuang@mail.ipc.ac.cn

Received 10 March 2021; Revised 4 June 2021; Accepted 13 July 2021; Published 23 July 2021

Academic Editor: Michael Aizenshtein

Copyright © 2021 Shuang Shuang et al. This is an open access article distributed under the Creative Commons Attribution License, which permits unrestricted use, distribution, and reproduction in any medium, provided the original work is properly cited.

SiB₆ powders were prepared by the “chemical oven” method from Si and B powders. Here combustion with acid pickling “two-step” mode replaces the traditional synthesis method which helps to avoid severe condition of high temperature and high pressure. It could realize maximum reaction temperature to about 2000°C, and the whole process just needs ~30 s. The average diameter of products is ~10 μm. And the raw material Si and B are ~3 μm and ~20 μm, respectively. The infrared emissivity of products was evaluated by UV-vis spectrum with absorption band around 250~2500 nm. All five samples show higher emissivity over UV-visible light range with lower emissivity over near-infrared range. Typically, the sample’s Si/B ratio of 1 : 1 shows highest integral intensity for about 0.85 compared with other molar ratios. It can be used as a more simple and effective method to obtain infrared ceramic SiB₆ with high emissivity.

1. Introduction

Infrared radiation coating could improve the emissivity of coating surface effectively [1, 2], enhancing the radiation heat transfer and achieving the purpose of energy saving. Thus, it shows a broad application prospect on the energy conservation of industrial kiln. High-emissivity infrared ceramic powders are the key to determine the properties of infrared radiation coatings. Nowadays, high-emissivity infrared ceramic powder under O₂ atmosphere is mainly the spinel oxide system. However, its service temperature is lower than 1300°C which is difficult to be used in high-temperature kiln. Also, SiB₆ is a good candidate as radiation substrate, which can be applied to infrared radiation coatings above 1300°C [3].

SiB₆ was first discovered in 1900 [4], when a mixture of silicon and boron was melted. The crystal structure of SiB₆ was initially reported to be cubic; however, it was later confirmed to be orthorhombic P_{nmm} [5]. Until now, there is no efficient method for synthesis of bulk SiB₆ samples.

Generally, the polycrystalline samples of SiB₆ should be prepared under high temperature and hot pressing. Si and B powders are usually weighed and mixed according to the measurement ratio and loaded into graphite mold lined with boron nitride (BN) to be hot-pressed into crystalline state at ~1600°C and ~4.0 × 10⁶ Pa. According to complex Si-B phase diagram, we know that the product is not always a single SiB₆ phase, and when hot-pressing was chosen, the elemental carbon solubility in SiB₆ could reach to about 2% (carbon in graphite mode will contaminate the sample). Thus, polycrystalline block composition and purity often do not meet the requirements.

Here the “chemical oven” method has attracted great attention due to its simple process, convenient operation, high yield, and easy industrialization, which has become a hot research topic for powder materials [6]. One recent work reported that Wang et al. have developed an ultrafast high-temperature sintering process for the fabrication of ceramic materials by radiative heating under an inert atmosphere. This kind of synthesis also belongs to a kind of “chemical

oven" [7]. Thus, inspired by this work, we propose to use a similar method for SiB_6 synthesis. The external reactant on the surface is ignited by high-energy heat input, and combustion occurs in a certain internal wave propagation rate of reactant particles. Then the inner reactant was also lit by external reaction heat. Transient superhigh temperature reduces reaction synthesis time. Jianguang Xu et al. have prepared a high pure molybdenum disilicide. And the product by "chemical oven" self-propagating high-temperature synthesis (SHS) method is more homogeneous than the normal SHS method. The whole process can be reacted in just a few seconds by the application of an electric field [6].

This method has been widely used to prepare high-temperature materials such as ceramics and intermetallic compounds [8–10]. Here we propose to use the high exothermic effect of reaction between reactants (Si and B powders) to make the chemical reaction maintain itself, so as to synthesize new materials.

2. Materials and Methods

The raw powders were mixed according to different stoichiometric ratios of Si/B. Here silicon's particle size is ~ 3 microns whose purity is 99.99% (Shanghai Aladdin Biochemical Technology Co. Ltd.). Also, boron's particle size is ≤ 20 microns with the purity of 99% (Shanghai Aladdin Biochemical Technology Co. Ltd.). Ball milling was adopted to mix the materials to ensure a homogeneous mixture, and ethanol was also added to wet grinding for 1 hour. The sample was dried in an oven over 110°C after taking out. They were then pressed into (10 MPa, maintaining 3 min) cylindrical pellets with a diameter of 15 mm.

Figure 1 shows inner structure of reaction oven. Here Ti, C, Al, and Fe_2O_3 were used as the thermite agents. The reaction was ignited in air through W coil in spiral shapes. Furthermore, we used tungsten-rhenium thermocouple to test inner reaction temperature curve, and here the sample was taken in a chemical oven with 65% ($2\text{Al} + \text{Fe}_2\text{O}_3 \rightarrow 2\text{Fe} + \text{Al}_2\text{O}_3$) + 35% ($\text{Ti} + \text{C} \rightarrow \text{TiC}$). According to the figure, the highest reaction temperature could reach 2000°C , with rapid heating rate of 27.6°C/s . As we all know, the melting point of Si is 1410°C . When heated higher than this, the solid Si turns to liquid Si, and the reaction between Si and B begins [11].

After reaction, the X-ray diffraction (XRD, D8 Focus, Bruker) and ultraviolet visible spectrum (UV-Vis, Cary-5000, Varian) of products were characterized. X-ray photoelectron spectroscopy (XPS, ESCALab220i-XL, VG) spectrum, EDS (S-4300, Hitachi), and scanning electron microscopy (SEM, S-4800, Hitachi) were also performed on the specimens cross sectional and broken powder for analysis of the microstructural characteristics. Table 1 presents the molar ratio of the silicon and boron powders used in this investigation.

3. Results and Discussion

Firstly, we changed different thermite ratios for exploring suitable reaction temperature as shown in Figure 2(a). Here

different ratios of $\text{Al}/\text{Fe}_2\text{O}_3 + \text{Ti}/\text{C}$ as exothermic reaction agent were set. They are 50%, 50%; 65%, 35%; 75%, 25%, respectively. With higher ($\text{Al} + \text{Fe}_2\text{O}_3$) ratio, reaction temperature will become higher. Thus according to XRD figure, when Ti/C ratio is 65%, SiB_6 presents as main phase with little SiB_4 and unreactive Si, B powder. So, here we adopt 65% as ($\text{Al} + \text{Fe}_2\text{O}_3$) ratio for next reaction parameter. This could realize maximum temperature about 2000°C , and the whole process just needs ~ 30 s.

Figure 2(b) shows the XRD patterns of different samples before and after acid pickling. All products after treatment exhibited diffraction peaks at 22.7° , 26.5° , 37.6° , 40.4° , 53.1° , and 55.7° corresponding to the (321), (411), (124), (551), (723), and (841) crystal planes of SiB_6 (JCPDS No. 35-0809) [12–14]. Besides this, the diffraction peak 34.4° of SiB_4 (021) (JCPDS No. 35-0777) can also be found in the XRD patterns [15]. Thus according to XRD figure, when Ti/C ratio is 65%, SiB_6 presents as main phase with little SiB_4 and unreactive Si, B powder. However, characteristic peaks of Si before acid pickling are very strong in all the samples in Supplement Figure 1. This is also the reason why we do the pickling treatment.

In situ XPS was also performed to verify the chemical binding state of samples after acid pickling from different Si/B molecular ratios. XPS surveys of all samples are shown in Figure 3(a). Figures 3(b)–3(d) are XPS spectra of O 1s, Si 2p, B 1s fine scan spectrum of Si/B=1:1 sample. The deconvolution peaks are displayed in Figure 3(b); O 1s spectrum was observed from 526.6 eV to 537.2 eV. The low binding energy (BE) component observed at ~ 531 eV corresponds to the main lattice oxygen (O_{lat}). The bands around ~ 533 eV can be assigned to adsorbed oxygen (O_{ads}) while the peak between them (~ 532 eV) indicates the ionization of oxygen species that could allow compensation for some deficiencies (O_{def}) connected in part to the variations in the concentration of oxygen vacancies in products [16]. The peak of Si at 99.1 eV is due to metallic Si^0 . The left peak can be divided into three peaks which are 103.6 eV, 102.8 eV, and 102.0 eV that can be referred to Si in (SiB_4), Si in (SiB_6), and SiO_x [17]. The area ratio is 1:1:1.06:1.37. The B 1s spectrum indicates that there are B atoms at the surface or subsurface of SiB_6 . In the B 1s spectrum, the peak at 187.5 eV is related to SiB_6 , while the peak at 186.8 eV attributes to SiB_4 [18]. And the area ratio is 1.03:1:1.10:1.

Figures 4(a)–4(d) show different magnification time pictures of typical top-view SEM images for Si/B=1:1 sample's cross section. The cylindrical sample was scraped for fresh cross profile. Here Figures 4(c) and 4(d) are enlarged views of white box in Figures 4(a) and 4(b). SiB_6 sintering piece shows brittle rupture from SEM. According to Figure 4(d), the average diameter of products is ~ 10 μm which is the between two raw materials' diameter (Si (~ 3 μm) and B (~ 20 μm) powder). These might be due to ball milling before sintering. EDS results focusing on Si, B, and O elements are also characterized which are shown in Supplementary Information Figure 2.

The diffuse reflectance UV-vis spectra of products are shown in Figure 5. Five samples exhibit absorbance over 250–2500 nm. Also, they show higher absorption over UV-visible light range with lower absorption over near-infrared range. When Si/B ratio decreases, the emissivity

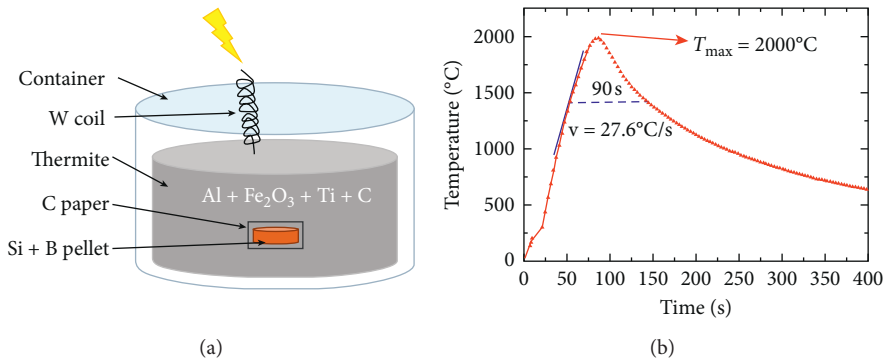


FIGURE 1: (a) Inner structure of chemical oven and its (b) temperature combustion curve with time.

TABLE 1: Molar ratio of Si : B for different samples.

Sample no.	Reaction ratio	
	Si ($3 \mu\text{m}$)	B ($\leq 20 \mu\text{m}$)
1	2	1
2	1	1
3	1	1.5
4	1	2
5	2	3

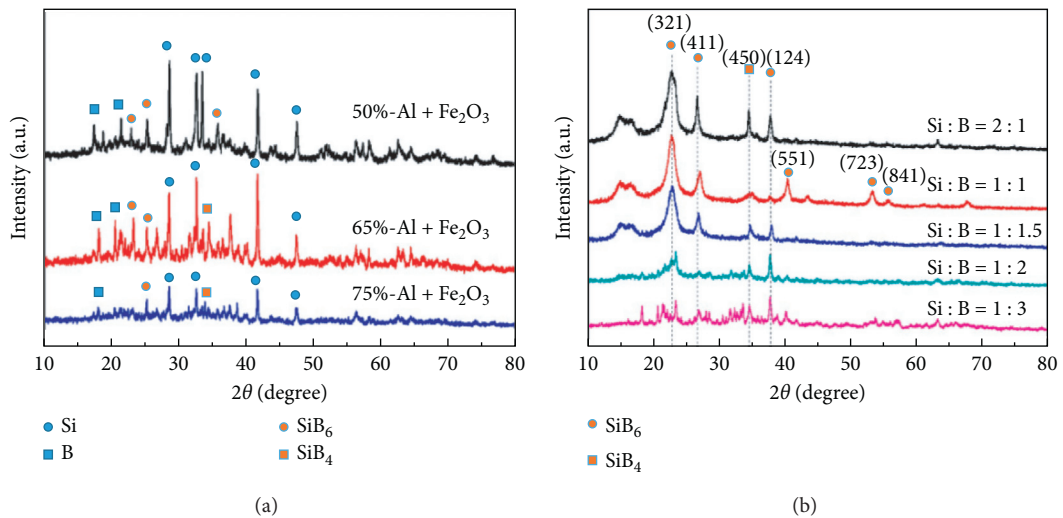


FIGURE 2: XRD spectrum of all samples (a) with different thermite ratios and (b) different molar ratios of Si/B.

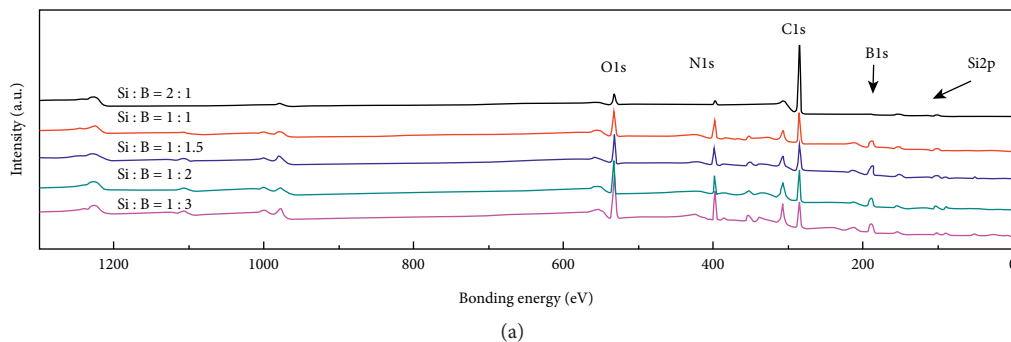


FIGURE 3: Continued.

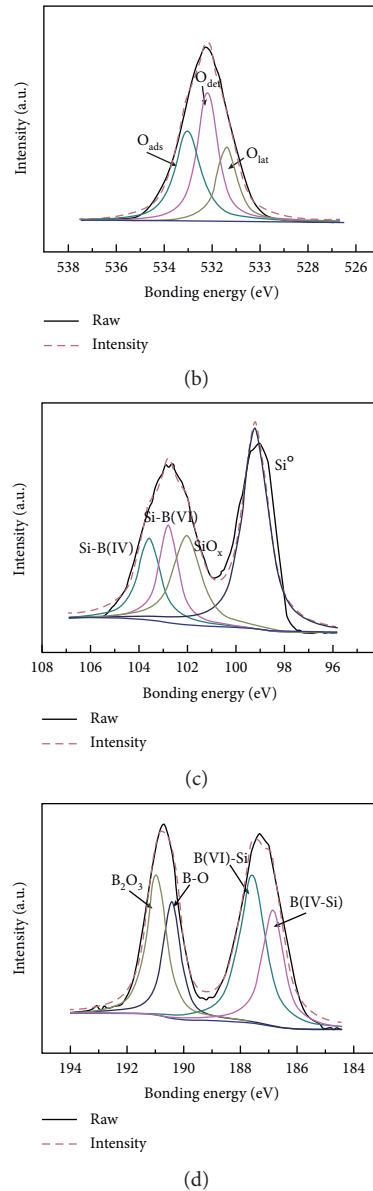


FIGURE 3: X-ray photoelectron spectroscopy (XPS) spectra of all samples: (a) survey of products; (b) O 1s; (c) Si 2p; (d) B 1s.

over UV-visible part increases and over NIR part decreases. Herein, Si/B ratio 1:1 shows highest integral intensity for about 0.85.

The band gap energy (E_g) of semiconductor, following the equation: $\alpha E_{\text{photon}} = K(E_{\text{photon}} - E_g)^{1/2}$, where K , α , E_{photon} and E_g are a constant; the absorption coefficient, the discrete

photon energy, and the band gap energy are estimated by calculating the intercept of an extrapolated linear fit to the experimental data of a plot of $(\alpha E_{\text{photon}})^2$ versus E_{photon} yielded E_g for a direct transition. As shown in Figure 6, the band gaps of samples molar ratio from 2 to 1/3 are figured out to be 1.73, 1.62, 1.75, 1.91, and 1.84 eV, respectively.

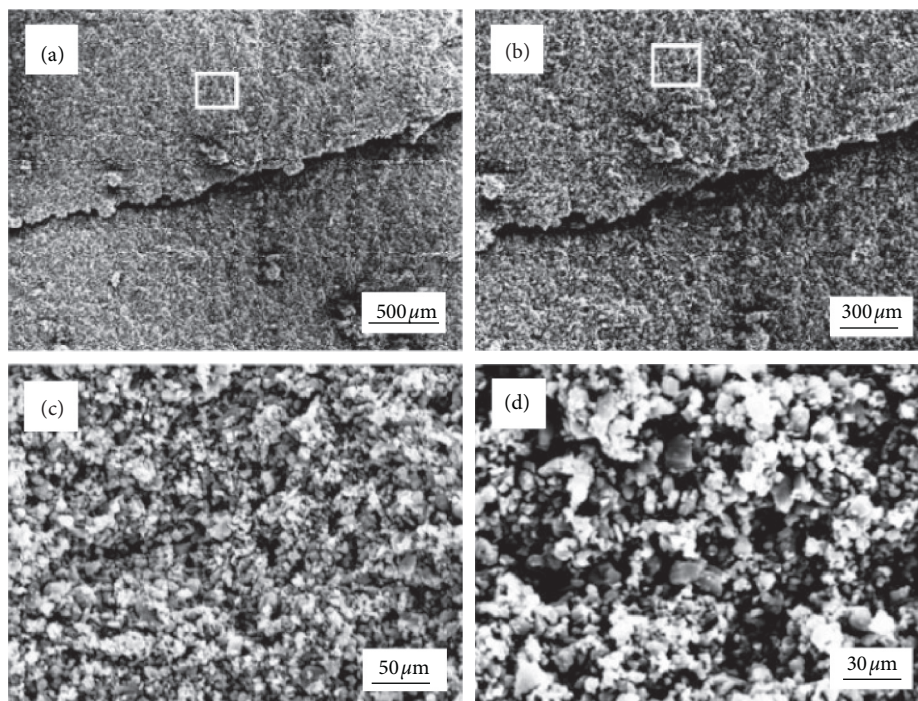


FIGURE 4: SEM images of the molar ratio of Si/B = 1:1 sample with different magnification time: (a) 150; (b) 300; (c) 500; (d) 1500..

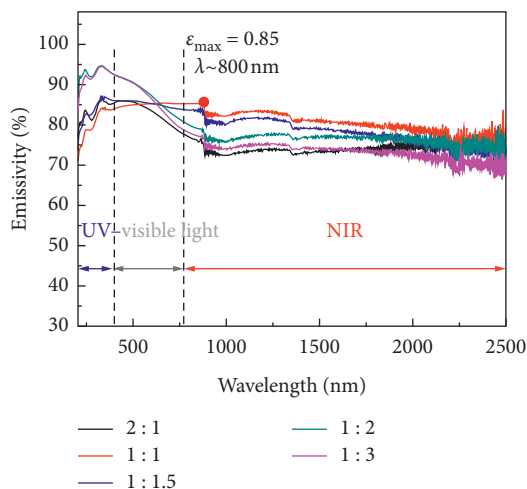


FIGURE 5: UV-vis emissivity spectra of all samples.

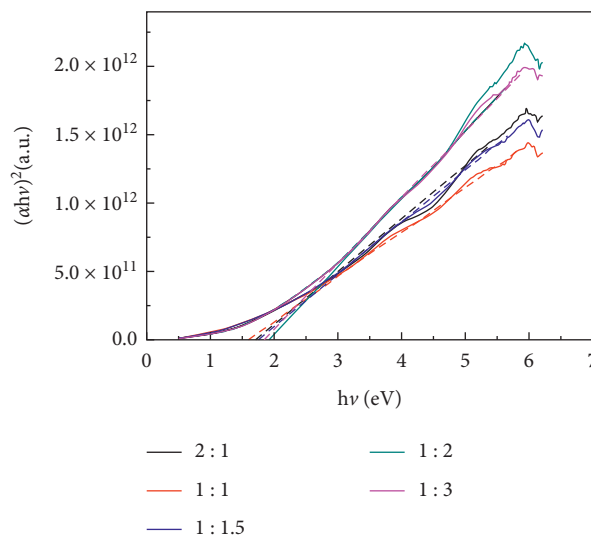


FIGURE 6: $(\alpha E_{\text{photon}})^2$ versus E_{photon} plots of all samples.

4. Conclusions

SiB₆ powders were prepared by the “chemical oven” method from Si and B powders. The external reactant on the surface is ignited by high-energy heat input, and combustion occurs in a certain internal wave propagation rate of reactant particles. After acid pickling, the products are obtained. Here SiB₆ is a dominant phase. The UV-vis diffuse reflectance obtained at different B/Si molar ratios from 0.5 to 1.5 are investigated. All five samples show higher absorption on UV-visible light range with lower absorption on near near-infrared range. What is more, when the ratio of Si/B decreases, the emissivity intense over

UV-visible part increases and intense over NIR part decreases. Herein, Si/B ratio 1:1 shows highest integral intensity for about 0.85. So, this product is expected to be used in high-temperature infrared radiation, and this method can be used as a more simple and effective method to obtain infrared ceramic SiB₆.

Data Availability

The data used to support the findings of this study are included within the article and supplementary information file.

Conflicts of Interest

The authors declare that there are no conflicts of interest regarding the publication of this paper.

Acknowledgments

This study was supported by the National Key Research and Development Program of China (no. 2016YFB0700204) and National Natural Science Foundation of China (nos. 51702331, 51572268, 51432004, and 51372255).

Supplementary Materials

Supplement Figure 1: XRD spectrum of products before acid pickling. Supplement Figure 2: EDS results of 1:1 molar ratio sample. (*Supplementary Materials*)

References

- [1] M. F. Passos, N. M. S. Carvalho, A. A. Rodrigues et al., "PHEMA hydrogels obtained by infrared radiation for cartilage tissue engineering," *International Journal of Chemical Engineering*, vol. 2019, Article ID 4249581, 9 pages, 2019.
- [2] J. Zheng, Y. Zhao, Y. Wang, S. Hu, P. Lu, and X. Shen, "The infrared radiation temperature characteristic of acupoints of mammary gland hyperplasia patients," *Evidence Based Complementary and Alternative Medicine*, vol. 2013, Article ID 567987, 2013.
- [3] J. Wu, W. Ma, B. Yang, D. Liu, and Y. Dai, "Calculation and characterization of silicon-boron phases in metallurgical grade silicon," *Silicon*, vol. 4, no. 4, pp. 289–295, 2012.
- [4] H. Moissan and A. Stock, "Ueber die beiden Borsiliciumverbindungen SiB_3 und SiB_6 ," *Berichte der Deutschen Chemischen Gesellschaft*, vol. 33, no. 2, pp. 2125–2131, 1900.
- [5] M. Vlasse, G. A. Slack, M. Garbaskas, J. S. Kasper, and J. C. Viala, "The crystal structure of SiB_6 ," *Journal of Solid State Chemistry*, vol. 63, no. 1, pp. 31–45, 1986.
- [6] X. Jianguang, Z. Baolin, L. Wenlan, Z. Hanrui, and J. Guojian, "Synthesis of pure molybdenum disilicide by the "chemical oven" self-propagating combustion method," *Ceramics International*, vol. 29, no. 5, pp. 543–546, 2003.
- [7] C. Wang, W. Ping, Q. Bai et al., "A general method to synthesize and sinter bulk ceramics in seconds," *Science*, vol. 368, no. 6490, pp. 521–526, 2020.
- [8] S. Zhang and Z. A. Munir, "Synthesis of molybdenum silicides by the self-propagating combustion method," *Journal of Materials Science*, vol. 26, no. 13, pp. 3685–3688, 1991.
- [9] J. Subrahmanyam, "Combustion synthesis of MoSi_2 - Mo_5Si_3 composites," *Journal of Materials Research*, vol. 9, no. 10, pp. 2620–2626, 1994.
- [10] S. C. Deevi, "Diffusional reactions in the combustion synthesis of MoSi_2 ," *Materials Science and Engineering*, vol. 149, no. 2, pp. 241–251, 1992.
- [11] S. J. Ikhmayies, "Thermo-calc determination of phase diagram of Si-B binary system," *Journal of Occupational Medicine*, vol. 73, no. 1, pp. 253–259, 2020.
- [12] J. F. Huang, Y. L. Zhang, and L. Y. Cao, *Microstructure and oxidation resistance of SiB_6 - MoSi_2 composite coating*, Journal of Shaanxi University of Science and Technology, Xi'an, China, 2014.
- [13] L. Weisheng, R. Xuanru, C. Hongao et al., "Preparation of MoSi_2 - SiB_6 oxidation inhibition coating on graphite by spark plasma sintering method," *Surface and Coatings Technology*, vol. 405, Article ID 126511, 2021.
- [14] M. N. Mirzayev, S. H. Jabarov, E. B. Asgerov et al., "X-ray diffraction and thermodynamics kinetics of SiB_6 under gamma irradiation dose," *Silicon*, vol. 11, no. 5, pp. 2499–2504, 2018.
- [15] H. F. Rizzo and L. R. Bidwell, "Formation and structure of SiB_4 ," *Journal of the American Ceramic Society*, vol. 43, no. 10, pp. 550–552, 1960.
- [16] J.-C. Dupin, D. Gonbeau, P. Vinatier, and A. Levasseur, "Systematic XPS studies of metal oxides, hydroxides and peroxides," *Physical Chemistry Chemical Physics*, vol. 2, no. 6, pp. 1319–1324, 2000.
- [17] M. Çopuroğlu, H. Sezen, R. L. Opila, and S. Suzer, "Band-bending at buried SiO_2/Si interface as probed by XPS," *ACS Applied Materials & Interfaces*, vol. 5, no. 12, pp. 5875–5881, 2013.
- [18] N. J. Kramer, K. S. Schramke, and U. R. Kortshagen, "Plasmonic properties of silicon nanocrystals doped with boron and phosphorus," *Nano Letters*, vol. 15, no. 8, pp. 5597–5603, 2015.